JOURNAL OF MATERIALS SCIENCE 26 (1991) 2184–2188

Discrete failure mode detection in a woven SiC cloth reinforced glass composite

J. W. KRYNICKI, R. E. GREEN Jr
Center for Nondestructive Evaluation, The Johns Hopkins University, Baltimore, MD 21218, USA

D. C. NAGLE
Martin Marietta Laboratories, Baltimore, MD 21227, USA

Single layer silicon carbide cloth reinforced glass composites were fabricated and subjected to three-point bending in order to develop better models of failure mechanisms. Acoustic emission (AE) monitoring was also performed during the bend tests to help isolate these mechanisms. During the basic flexural tests, discrete failure modes, which were often not visible from specimen surfaces, displayed their existence through characteristic load–deflection curve unloading regions and abrupt changes in acoustic activity. Microscopic three-point bend tests were then performed to elaborate on the results of the conventional bend tests. Observations made during the microscopic bend tests provided a one-to-one correlation with load–deflection curve anomalies and acoustic emission activity. As a result of the different mechanical, optical and acoustical techniques used, discrete failure mechanisms for the cloth reinforced ceramic matrix composite (CMC) were conclusively established.

1. Introduction

The addition of reinforcing fibres to ceramics has proven to be the most effective method for toughening inherently brittle ceramics. While the earliest ceramic matrix composites used continuous fibre layups for reinforcement, the use of woven cloth has become increasingly popular. Consequently, since the use of woven cloth in ceramic composites is relatively novel, a detailed understanding of fracture mechanisms for this type of composite is not presently known. For any fibre-reinforced ceramic–matrix composite, the quality of the interface is critical. Unlike metal and polymer based composites which require the strongest possible bond between the matrix and fibre reinforcement, ceramic composites are dependent upon mechanical keying between its components and weak interfacial bonding. The consequence of too strong a chemical bond is that it causes a propagating crack to not "see" the fibre and causes the material to behave as a monolithic brittle ceramic. Through the presence of strong mechanical keying and strain relief mechanisms such as fibre pull-out, it is hoped that the ceramic matrix composite will fail in a non-catastrophic manner. This graceful failure is typically accomplished by the development of multiple strain relief mechanisms during loading. The significance of multiple strain relief mechanisms in unidirectionally reinforced ceramic composites was investigated in detail by Aveston *et al.* [1].

Flexural tests on continuous fibre reinforced ceramic matrices have often exhibited non-catastrophic failure and load–deflection curves that expressed a "saw-tooth" behaviour resulting from random microcracking. Other tests have shown smoother curves that still contained either some type of "saw-tooth" behaviour or a "blip" [2]. Even with the aid of an optical microscope (400 × magnification), cracks were often not observed even after "blips" in the load–deflection curve were observed. Mah and Mendiratta [3], found both modes of principal failure, compressive and tensile, depending on the matrix used in the composite. Meanwhile, other studies have discussed how during loading, unidirectional CMCs develop regularly spaced microcracks which bridge fibres [4].

While it would be inaccurate to believe that the failure mechanisms observed by Mah and Mendiratta were identical to those of the single layer SiC–7740 system used in this study, discrete failure modes were indeed observed when the specimen was evaluated through various techniques. A study performed by Krynicki [5] revealed results similar to those of Mah and Mendiratta in that during three-point bend tests of a single layer CMC, "steps" found in the load–deflection curve did not always provide a one-to-one correlation with dye penetrant or microscopic surface inspection for cracks. Fig. 1 taken from Krynicki shows load–deflection curve anomalies in a single layer CMC.

Acoustic emission is the release of a transient elastic wave through a strain relief mechanism. While the behaviour of elastic waves in any material are heavily influenced by many things such as multimode, multifrequency signals, geometrical spreading, geometrical scattering, source geometry and contact acoustic detection devices, relative changes in acoustic emis-

0022–2461/91 $03.00 + .12

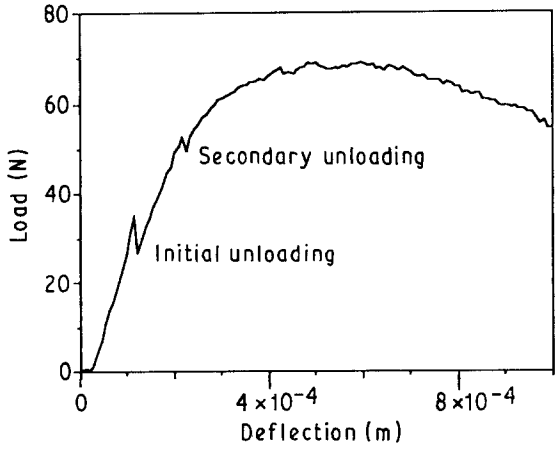

Figure 1 Load–deflection curve from a single layer CMC subjected to three-point bending. Taken from Krynicki [5].

sion activity has long been a viable technique for monitoring structural integrity during mechanical loading of many types of materials, especially fibre-reinforced plastics [6–9].

A common technique for using acoustic emission as a measure of released strain energy has been the use of total AE counts, also referred to as ring-down counting. Ring-down counting is simply a count of the number of times the sensor voltage of an AE signal exceeds a fixed voltage threshold.

Regarding unidirectionally reinforced ceramics, several authors have correlated acoustic activity with crack propagation during mechanical loading [10–12]. Work by Noone *et al.* [12] proved some relations existed between subcritical cracks and acoustic emission in a CMC, yet for the unidirectionally reinforced material used in their study, fracture mechanisms did not develop in a predictable manner.

2. Experimental procedure

The composite manufactured in the present study was composed of a Corning class 7740 borosilicate glass powder with a Nicalon silicon carbide woven cloth as the reinforcement. The Nicalon cloth was a two-dimensional woven roving comprised of equal fibre fractions in mutually perpendicular directions. The composite was formed in a fine grained graphite mould. Before placing any of the composite's constituents in the mould, the mould was painted with a graphite emulsion to facilitate the removal of the manufactured composite after processing. After coating the graphite mould, a glass slurry was poured into the mould. The Nicalon matte was then placed on top of the first glass layer. Lastly, a final layer of the glass slurry was poured onto the SiC matte. The composite was then hot-pressed at approximately 1100 °C. The resulting fibre volume fraction was calculated to be approximately 9%. Using a small volume fraction in this study allowed a more direct interpretation of experimental results. As a control for the CMC, a non-reinforced glass specimen was also hot-pressed. After manufacture, average theoretical densities of 95.0 and 95.5% were determined for the reinforced and non-reinforced specimens, respectively.

Coupon specimens were cut from the hot-pressed CMC composite samples in a manner so that one of the mutually perpendicular predominant fibre directions would be perpendicular to the loading noses, therefore, 50% of the fibre volume fraction was always perpendicular to the loading noses while the other 50% was parallel to the noses. Specimens were typically 30 mm wide by 2.25 mm thick. Non-reinforced specimens of similar dimensions were also cut. In order to normalize surface defect effects, the specimens' faces were lightly abraded using a 500 grit, 30 μm, silicon carbide paper.

The support span of the three-point testing jig was 25.4 mm and the loading noses possessed a 3.2 mm radius (Fig. 2). A sufficient amount of overhang was provided for the specimen. An Instron screw type loading machine Type TT-CM was used to provide a constant deflection rate of 0.2 mm min^{-1} for all tests performed in this study. Load cell amplification was conducted by a Measurements Group model 2310 Signal Conditioning Amplifier. The amplified signal was then sent to an acoustic emission monitoring device for storage. Load cell calibration curves were performed in a conventional manner yielding highly linear and repeatable load–voltage curves.

In order to determine an optimal frequency band for the acoustic emission monitoring, a step response unloading (representative of white noise) was performed on the specimen and then monitored through a broadband detector. Since one generally does not know the frequency content of signals detected during acoustic emission monitoring, a judicious choice must

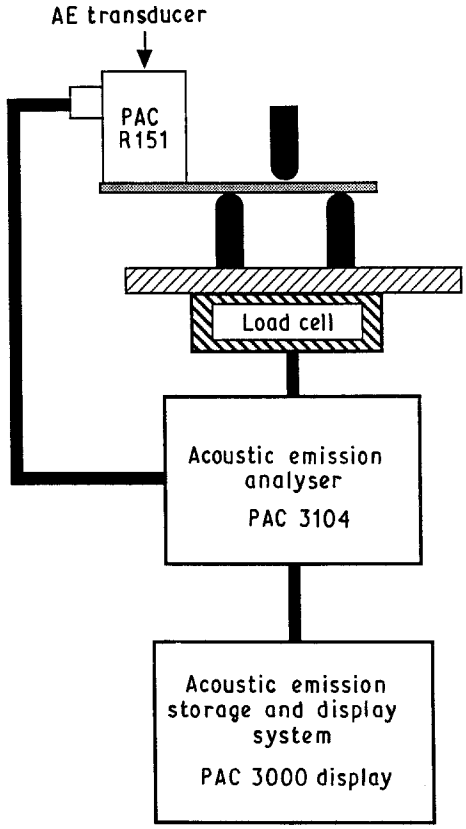

Figure 2 Schematic of three-point bend test and acoustic emission instruments.

be made in determining the optimal frequency bandpass for piezoelectric transduction. For example, while minimizing electronic and background mechanical noise, the bandpass must be wide enough to include high frequency signals which often reveal information regarding rapid crack growth and low frequency signals which are indicative of frictional mechanisms such as fibre pull-out.

As put forth by Hsu [13], a pencil lead break was performed on the specimen's surface to simulate an acoustic emission spike. Broadband signal detection ($\approx$ 45 kHz to 3 MHz) was possible through the use of a Valpey Fisher Pinducer (a small piezoelectric transducer), along with signal amplifiers and a digital oscilloscope. The frequency response of the pencil lead break revealed that most of the detectable acoustic energy for the specimen used in this study was between 50 and 650 kHz. By analysing the frequency domain of the detected signal, an upper detection frequency was determined. In practice, apart from transducer response, the upper frequency limit for signal detection is limited by the increase in scattering and absorption which accompanies shorter wavelength (higher frequency) signals. In contrast, the lower frequency cut-off is typically limited by background frictional or mechanical noise, and again, transducer response.

Using the information found during the pencil lead break, a piezoelectric transducer best suited for this study was chosen. The transducer was a Physical Acoustics R151 Integral transducer with a detection band of 100 to 450 kHz and a resonant frequency of 160 kHz. The transducer, possessing a self-contained 40 dB amplifier, was acoustically coupled through silicon grease and then securely fastened to the sample with tape (Fig. 2). The use of this relatively high frequency transducer allowed the filtering of extraneous background mechanical noise. The transducer output was then sent to a Physical Acoustics 3000/3104 AE monitoring system for signal amplification, digitization, storage and manipulation. Using a total gain of 60 dB (40 dB from the transducer and 20 dB from the main amplifier), a threshold of 0.2 V was set to provide a sufficient threshold above background noise. Signal dead time was set to 40 ms. Data were stored at a rate which provided a one second resolution. Acoustic emission data were displayed as the average number of counts per event during a 1 s interval.

In order to elaborate upon load–deflection curve anomalies and corresponding acoustic emission results, microscopic three-point bend tests as depicted in Fig. 3 were performed. These were performed by cutting narrow sections from the hot-pressed specimens and then bending them in a small test fixture under a light microscope. This work was performed under a magnification of 32 $\times$.

3. Results and discussion

Results of the acoustic emission monitored bend tests shown in Fig. 4 did indeed suggest discrete failure modes in the cloth reinforced composite. However, apart from the two separate highly pronounced strain relief mechanisms, which were present during the bending of the CMC, little else could be inferred. Therefore, microscopic bend tests of this CMC, possessing an optically transparent matrix, were warranted in order to elaborate upon the standard flexural test.

Utilizing the three investigative tools combined in this study, (flexural testing, acoustic emission and optical microscopy), the entire failure of the composite can be summarized in four steps which are listed under the following subheadings. The first three subheadings are the composite's primary failure modes and these are shown schematically in Fig. 5.

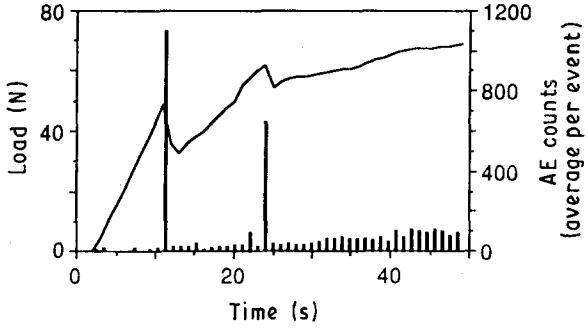

Figure 4 Load and average AE counts plotted against time (deflection) for a single layer CMC.

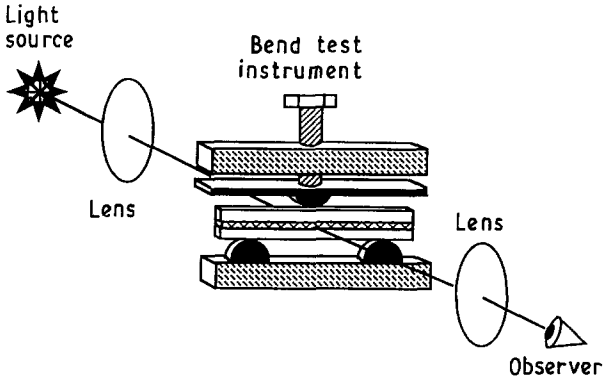

Figure 3 Schematic of microscope and bend test instrument.

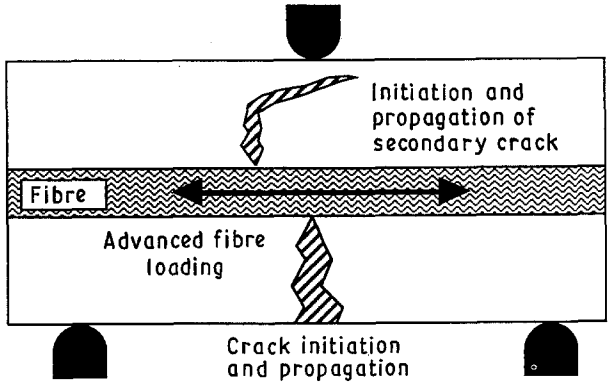

Figure 5 Schematic representation of failure modes during three-point bend test of a single layer CMC.

3.1. Crack initiation and propagation

A crack rapidly propagates from the tensile side up to the fibre–matrix interface. This first crack is also shown in a photomicrograph (Fig. 6). As one might expect, Fig. 4 reveals that the specimen released no significant acoustic emission prior to the first load–deflection curve peak since the composite was behaving in an elastic fashion. Once the first tensile crack was initiated, however, a very sharp acoustic response was recorded ($\approx 10^3$ over background activity). A similar observation of acoustic emission activity was made for the loading of non-reinforced glass (Fig. 7).

3.2. Advanced fibre loading

Subsequent loading after the first failure yielded no further visible cracks, yet acoustic emission activity increased. It was believed that the additional loading was largely taken up by the tensile stressing of the fibres. This resulted in a complementary compressive field being developed in the upper portion of the glass composite. The manifestations of fibre stressing due to fibre pull-out is demonstrated by the upward slope of acoustic activity between the first and second peaks of the load–deflection curve. More specifically, this acoustic activity is attributed to frictional noise.

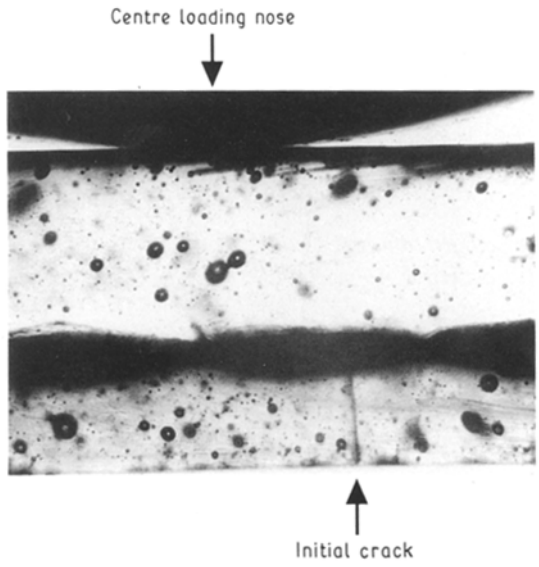

Figure 6 Photomicrograph of the initial failure mechanism for a single layer CMC subjected to three-point bending.

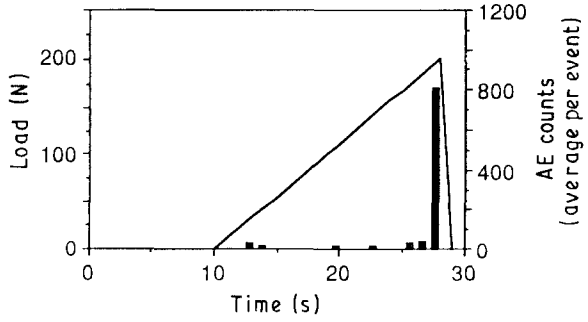

Figure 7 Load and average AE counts plotted against time (deflection) for a non-reinforced glass specimen subjected to three-point bending.

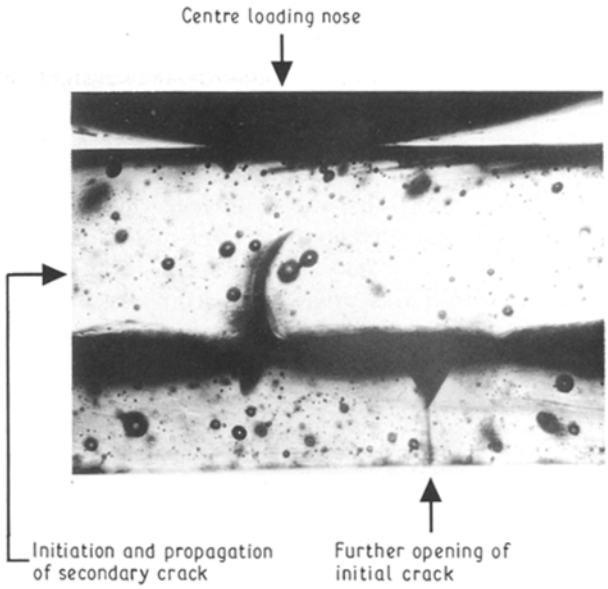

Figure 8 Photomicrograph of basic failure mechanisms for a single layer CMC subjected to three-point bending.

3.3. Initiation and propagation of secondary crack

Upon further loading, a crack was observed to initiate at the fibre–matrix interface which was originally in axial compression (Fig. 8). This second crack rarely originated directly opposite the tensile side crack. Thus, the fibres deflected the crack and impeded crack propagation. This second tensile crack, which originated at the interface, was expected since the neutral stress plane had moved up and placed the upper fibre–matrix interface in tension. The second tensile crack propagated very slowly towards the upper, (compressive side) loading nose, yet, this second crack was eventually deflected laterally from the loading nose since a sizeable compressive field existed immediately in front of the nose. Initiation of the second crack also caused a sharp increase in acoustic emission. The steady increase in acoustic activity after the second peak was attributed to the propagation of the second crack and addition frictional noise generated by fibre pull-out and fracture.

3.4. Advanced failure

As the specimen was further loaded, additional microcracks originated at locations near those of the first and third crack types and behaved accordingly. This additional microcracking and fibre pull-out again led to the increasing acoustic activity which was observed.

4. Conclusions

Discrete and predictable failure mechanisms for a single layer SiC cloth reinforced glass composite subjected to flexure were clearly identified. Strain relief mechanisms were first observed through

load–deflection curve anomalies. Acoustic emission monitoring of the three-point bend test along with microscopic bend tests provided detailed insight for failure modes of the single layer ceramic composite. The cumulative results of using these three evaluation techniques provide insight on how CMCs fail in general. It was shown that shortly after the initial tensile side crack propagated up to the fibre–matrix interface, a second crack would initiate at the fibre–matrix interface which was originally in compression. This interface was eventually placed in tension through a fibre pull-out mechanism. Since the second crack did not immediately propagate to the surface and the first one closed up as the load on the composite was removed, cracks were difficult to detect from typical visual surface inspection. While the exact location or magnitude of a crack can rarely be given solely by acoustic emission monitoring, the simple existence of a crack can be determined through its release of acoustic energy.

Ceramic matrix composites are often excellent candidates for high temperature applications. A CMC may, however, encounter degradation in an oxidizing atmosphere as many reinforcing fibres are susceptible to oxidation at elevated temperatures. A composite with a microcracked matrix may, therefore, allow oxygen to reach reinforcing fibres and then tunnel along fibres, thereby leading to material degradation. It is then proposed that acoustic emission monitoring during proof loading or *in situ*, would help indicate the potential for fibre degradation from chemical attack, since AE can describe the extent of matrix microcracking.

Even though the predictable failure modes found in this single layer composite will probably not be as evident in a more complex multilayer CMC, it is hoped that the predictable failure mechanisms found in this study can be applied to models of more complex CMCs. Through the understanding of failure mechanisms in cloth reinforced CMCs, better composite design systems will be achieved.

Acknowledgements

This work was supported by both The Johns Hopkins University Center for Nondestructive Evaluation and Martin Marietta Laboratories.

References

1. J. AVESTON, G. A. COOPER and A. KELLY, The Properties of Fiber Composites: Conference Proceedings, National Physical Laboratory, **4** (November 1971) pp. 15–26.
2. T. MAH and M. G. MENDIRATTA, *J. Amer. Ceram. Soc.* **68** (1985) C-27-C-30.
3. *Idem., ibid.* **68** (1985) C-29.
4. J. AVESTON and A. KELLY, *J. Mat. Sci.* **8** (1973) 352–362.
5. J. W. KRYNICKI, MSc Essay, Johns Hopkins University, Baltimore, MD (1989)
6. S. R. BUXBAUM, R. E. GREEN, Jr. and R. B. POND, Jr., *Nondestructive Testing Commun.* **1** (1984) 205–218.
7. M. A. HAMSTAD, *J. Acoustic Emission* **1** (1982) 151–164.
8. M. FUWA, B. HARRIS and A. R. BUNSELL, *J. Phys. D:* **8** (1975) p. 1460–1471.
9. J. M. CARLYLE, MTech Dissertation, Brunel University, Uxbridge, UK (1974).
10. D. J. LLOYD and K. TANGRI, *J. Mater. Sci.* **9** (1974) 482–486.
11. J. LANKFORD, Proceedings of the Fifth International Conference on Composite Materials, San Diego, CA, July 29-August 1, 1985, pp. 587–602.
12. M. J. NOONE and R. L. MEHAN, Proceedings of the Symposium on Fracture Mechanics of Ceramics, University Park, PA, July 11–13 1973, **1**, pp. 201–229.
13. N. N. HSU and S. C. HARDY, *AMD-* **29** (1978) 85–106.

Received 30 January
and accepted 2 August 1990